

LARGE EDDY SIMULATION OF THE NEAR WAKE OF A HEATED SPHERE AT $Re=10,000$

Matthew B. de Stadler¹ and Sutanu Sarkar²
Mechanical and Aerospace Engineering Department
University of California San Diego
9500 Gilman Drive #0411, La Jolla, CA 92093
mdestadl@ucsd.edu¹, sarkar@ucsd.edu²

ABSTRACT

Large eddy simulation is used to numerically simulate flow past a heated sphere at $Re=10,000$. A second order accurate in space and time, semi-implicit finite difference code is used with the immersed boundary to represent the sphere in a Cartesian domain. Visualizations of the vorticity field and temperature field are provided together with profiles of the temperature and velocity fields at various locations in the wake. The laminar separated shear layer was found to efficiently transport temperature from the hot sphere surface to the cold fluid in the wake. Pronounced Kelvin-Helmholtz induced rollers are formed which destabilize the separated shear layer and promote mixing. Calculations of the wake dimensions showed that the wake dimensions of the velocity field and the temperature field differ by 10% in the developed region behind the re-circulating region.

Introduction

Scalar mixing is important for a large number of practical situations from industrial applications to the detection of underwater vehicles to mixing and transfer of energy and contaminants in the ocean and atmosphere and others as noted by Berajeklian & Mydlarski (2011). Despite the practical importance of this flow, the literature for scalar mixing in the wake of three-dimensional bluff bodies is rather limited. Significantly more work has been done for the case of a cylinder wake, see for example Berajeklian & Mydlarski (2011), Matsumura & Antonia (1993) and references therein. Here we will discuss the relevant literature on three-dimensional bluff-bodies. Gibson *et al.* (1968) performed the first study of scalar mixing in the wake of a sphere by performing water tunnel measurements. The scalar field was added by a jet of hot water from the back of the sphere into the re-circulating region. They measured and obtained power law fits for the decay of the mean temperature, temperature variance, and scalar dissipation in the region $3 < x/D < 60$. In wind-tunnel experiments with an optically heated sphere at $Re = 4,300$, Freymuth & Uberoi (1973) observed self-similarity of the mean temperature and temperature variance for $x/D > 80$. The temperature excess was found to scale as $T \sim x^{-2/3}$ and the length scale as $l_T \sim x^{1/3}$. They also quantified the terms of the scalar variance budget where they observed strong convection and dissipation. They also observed self-similarity in one-dimensional temperature spectra and the presence of a $k^{-5/3}$

region with an increasingly large inertial range as Reynolds number increases. The very late wake of a heated sphere and the transition to the final decay period of turbulence was considered experimentally by Freymuth (1975) and theoretically by Freymuth (1976).

In wind-tunnel studies with a 6:1 ellipsoid with a hot jet of air emitted from the back of the body, Dmitrenko *et al.* (1986a) measured the relationship between the mean and fluctuating velocity and temperature fields in the wake. The data from Dmitrenko *et al.* (1986a) was used by Dmitrenko *et al.* (1986b) to measure cross-correlations of the velocity and temperature fluctuations as well as the terms in the temperature variance balance equation. Important results from these studies include: the thermal field has a finer scale than the velocity field, the mean temperature reaches self-similarity before the temperature fluctuations, the growth rate of the thermal wake width appears to be universal for axisymmetric bodies, temperature fluctuations increase as velocity fluctuations decrease and vice-versa. Dmitrenko *et al.* (1986a) found that the ratio of length scales between the velocity and temperature field was constant for both mean and fluctuating profiles for the entire wake evolution despite the thermal wake not exhibiting self-similarity.

Results from studies of scalar mixing in the wake of axisymmetric bodies are not universal. One of the principal results of Dmitrenko *et al.* (1986b) is that the shape of the body significantly affects the physical processes governing the evolution of scalar variance. Also, Berajeklian & Mydlarski (2011) showed that even for the same velocity field, flow statistics are sensitive to the method of scalar injection.

Formulation

We consider spatially-evolving flow past a stationary heated sphere in a fixed computational domain. The sphere is weakly heated so that temperature can be treated as a passive scalar. Our setup is the computational equivalent to a wind tunnel where undisturbed inflow enters the computational domain and flow exits through an outflow boundary. Suitable far-field boundary conditions are applied in the cross-stream directions to prevent blockage and end effects from contaminating the simulation.

High resolution LES is used to simulate the three-dimensional, unsteady, incompressible, Navier-Stokes equations subject to the Boussinesq approximation. For the LES, a standard Smagorinsky model is used for the sub-grid scale stress and buoyancy flux. As was done by Schmid

Table 1: Grid parameters. Here L_i represents the grid length in a given direction and n_i the number of grid points in the given direction. Note that the domain length given here does not include the additional size of the sponge region.

L_1	L_2	L_3	n_1	n_2	n_3
21.00	10.64	10.64	1024	576	576

& Peric (2001), a Smagorinsky coefficient of 0.1 was selected for this study. The governing equations are solved on a Cartesian grid with the immersed boundary method used to represent the sphere inside the domain. A Cartesian grid was chosen as we are more interested in the wake dynamics than in the near sphere flow field; such an approach was used by Parnaudeau *et al.* (2008) for flow past a cylinder. The grid used is a tensor product of three one-dimensional grids; grid stretching is used in all directions to concentrate points on the sphere to resolve the laminar boundary layer and to capture the details of the separated laminar shear layers.

The numerical method used is a semi-implicit combination of third order Runge-Kutta (RK3) for convective terms and second order alternating direction implicit (ADI) with a pressure correction algorithm for the viscous and pressure gradient terms. Second order centered differences are used for all spatial derivatives. The method is a combination of the low-storage RK3 method of Williamson (1980), with the unconditionally stable ADI method of Douglas (1962), and the pressure correction algorithms of Zang *et al.* (1994) and Rhie & Chow (1983). A flexible semi-coarsened multigrid solver is used for the pressure projection. Grid stretching in all 3 directions requires the use of a more robust multigrid solver able to handle different levels of anisotropy throughout the computational domain, a modification of the method of Piquet & Vasseur (2000) is employed. Lines are performed in the stream-wise direction and coarsening is performed in the other two directions. Unlike Piquet & Vasseur (2000) who use a Galerkin coarse grid approximation, here we apply a direct coarse grid approximation. A pipelined Thomas algorithm is used to efficiently solve the tridiagonal system of equations generated by ADI.

The direct forcing immersed boundary method of Roman *et al.* (2009) is used. This implementation decouples fluid and solid nodes, allows for a sharp interface at the boundary and requires only a single solution of the momentum equation at each substep.

Simulation parameters

Simulations are performed at a Reynolds number of 10,000 and a Prandtl number of 1. For this study, all values given are provided in their normalized form where normalization uses the sphere diameter D , the free stream velocity U_∞ , and the initial temperature difference between the sphere and the background ΔT_0 . The computational grid details are given in Table 1. The center of the sphere is located at $[0, 0, 0]$ with the inflow boundary at $x_1 = -5.0D$. A fixed timestep of $\Delta t = 0.00275$ is used; this value corresponds to a CFL number slightly less than 1. A sub-grid scale Prandtl number of 1 was chosen so that $\kappa_{sgs} = \nu_{sgs}$.

Stress-free boundary conditions are applied at the top, bottom and side boundaries. Uniform undisturbed inflow is applied at the inlet and linear extrapolation together with a sponge region are applied at the outflow boundary to allow flow to smoothly transition out of the domain. A no-slip boundary condition is applied for the velocity at the sphere and the temperature at the sphere boundary is fixed at a constant value, $\Delta T = 1$. Data from a simulation of flow past a sphere at $Re = 3,700$ is interpolated to the current grid for use as an initial condition.

18432 CPU hours on 288 processors were required for this study, see appendix for details of the machine used. Averaging was performed using data from six shedding cycles.

Validation

Validation of the flow is performed with available data from previous numerical and experimental studies at $Re = 10,000$ in Table 2. Good agreement is observed in the pro-

Table 2: Comparison of present data with that from previous numerical and experimental studies of the wake of a sphere at $Re = 10,000$. C+S refers to Constantinescu & Squires (2003); comparable statistics are also provided using DES in Constantinescu & Squires (2004).

	St	ψ_S	$\overline{C_{pb}}$	L_r/D
Present study	0.185	85-95	-0.262	1.724
Rodriguez <i>et al.</i> (2013) (DNS)	0.195	84.7	-0.272	1.657
Yun <i>et al.</i> (2006) (LES)	0.17	90	-0.274	1.364
C+S (LES)	0.195	84-86	-0.27	1.74
Achenbach (1974) (exp.)	0.148	-	-	-
Cometta (1957) (exp.)	0.195	-	-	-

vided statistics, note St is the Strouhal number, ψ_S is the separation angle, $\overline{C_{pb}}$ is the back pressure coefficient and L_r is the recirculation length. The mean pressure coefficient around the sphere was also found to agree well as shown in Figure 1. Considerable uncertainty was observed in the separation angle due to the mismatch of the computational grid and the sphere surface combined with interpolation error. In addition to reasonable agreement for the shedding frequency, we also observe a low frequency peak ($f < 0.04$, not enough data was present to determine the value) and a secondary peak corresponding to Kelvin-Helmholtz shedding as observed by previous studies.

Visualization of the vorticity and temperature fields

In Figure 2, we illustrate the connection between the vorticity field and the temperature field in the wake of the heated sphere. There is good agreement between the behavior of the vorticity and the temperature field. The temperature value is large in the re-circulating region immediately behind the sphere as expected. However, we can clearly

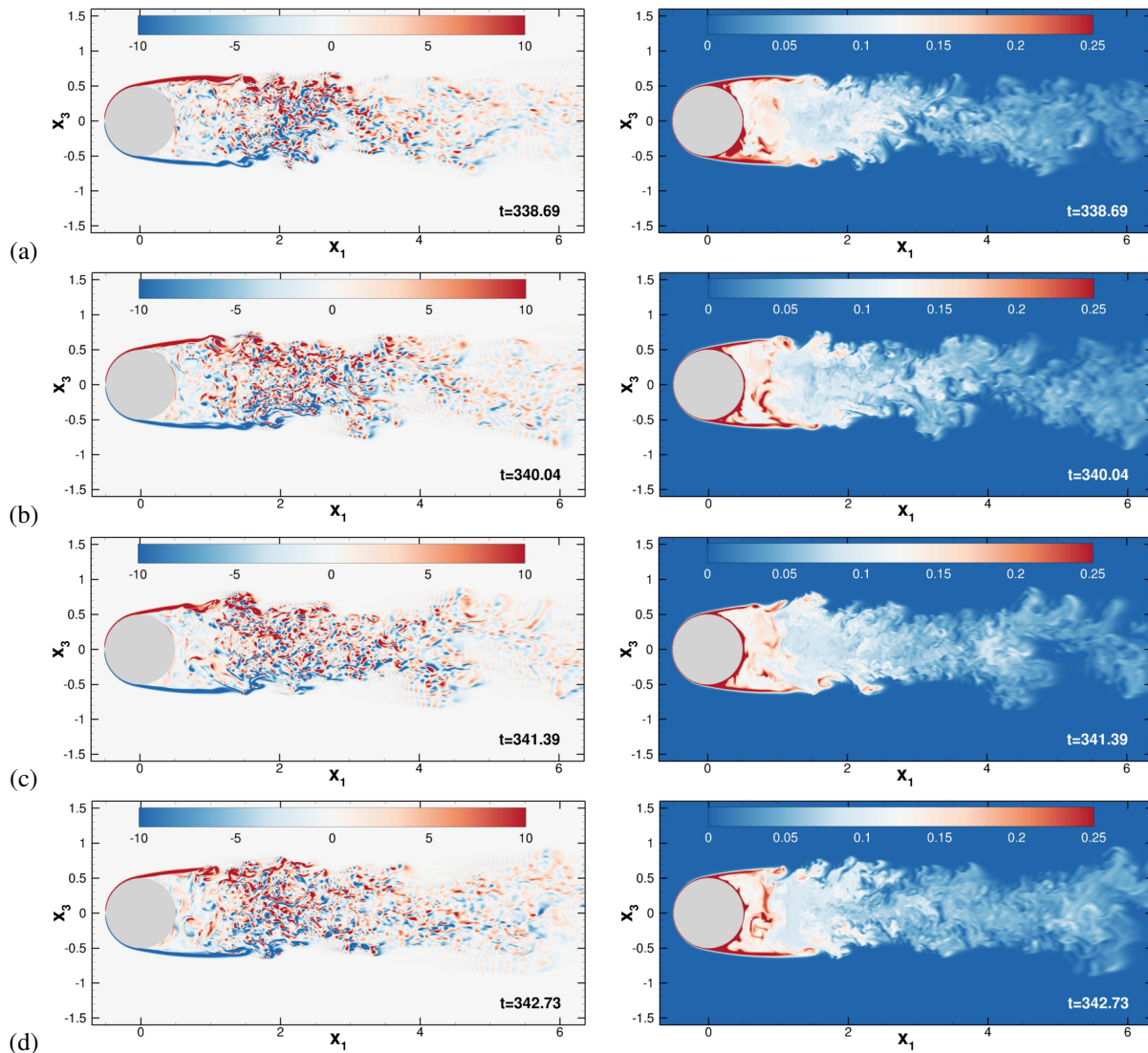


Figure 2: Instantaneous contours of the spanwise vorticity ω_2 (left column) and temperature field (right column). (a) The four images are shown at a time spacing of $1/4$ of a shedding period with time increasing from top to bottom. Note that due to the rapid decay of the temperature, a lower contour limit is chosen to illustrate the temperature distribution in the wake.

see that fluid is being transported from the sphere surface to the wake through the separated shear layer. Large values of both vorticity and temperature are seen in these thin separated layers. The vortex roll up is evident in the vorticity field and the rollers can be observed in the temperature field as well. These rollers enhance mixing by entraining cold fluid into the hot wake region. A secondary peak in the temperature field can be seen in the region in between the two shear layers at $x/D \approx 0.8$. This secondary peak is caused by swirling motions in the re-circulating region.

Mean and fluctuating statistics in the wake

Profiles of the mean and fluctuating velocity and temperature field are provided at five locations in the wake in Figure 3. The thin separated shear layers in the near wake can be seen in all four images at $x_1/D = 1.0$. By $x_1/D = 2.0$ the mean streamwise velocity field has transitioned to a Gaussian shape which is retained for the rest of the flow evolution. The mean temperature field transitions

to a Gaussian profile slightly later in time with evidence of the presence of the shear layers still retained at $x_1/D = 2.0$. The rms fields of the streamwise velocity and temperature are qualitatively similar. Both show a double-humped profile in the early wake before transitioning to what appears to be more of a flat-topped profile at intermediate time. The double-humped profile persists further in x_1/D for the fluctuating fields than for the mean fields.

Wake dimensions

The size of the wake for the velocity field and the temperature field can be quantified by calculating the wake dimensions. The wake dimensions are shown in Figure 4. Here the second order spatially centered moment definition of Brucker & Sarkar (2010) is used where the wake length

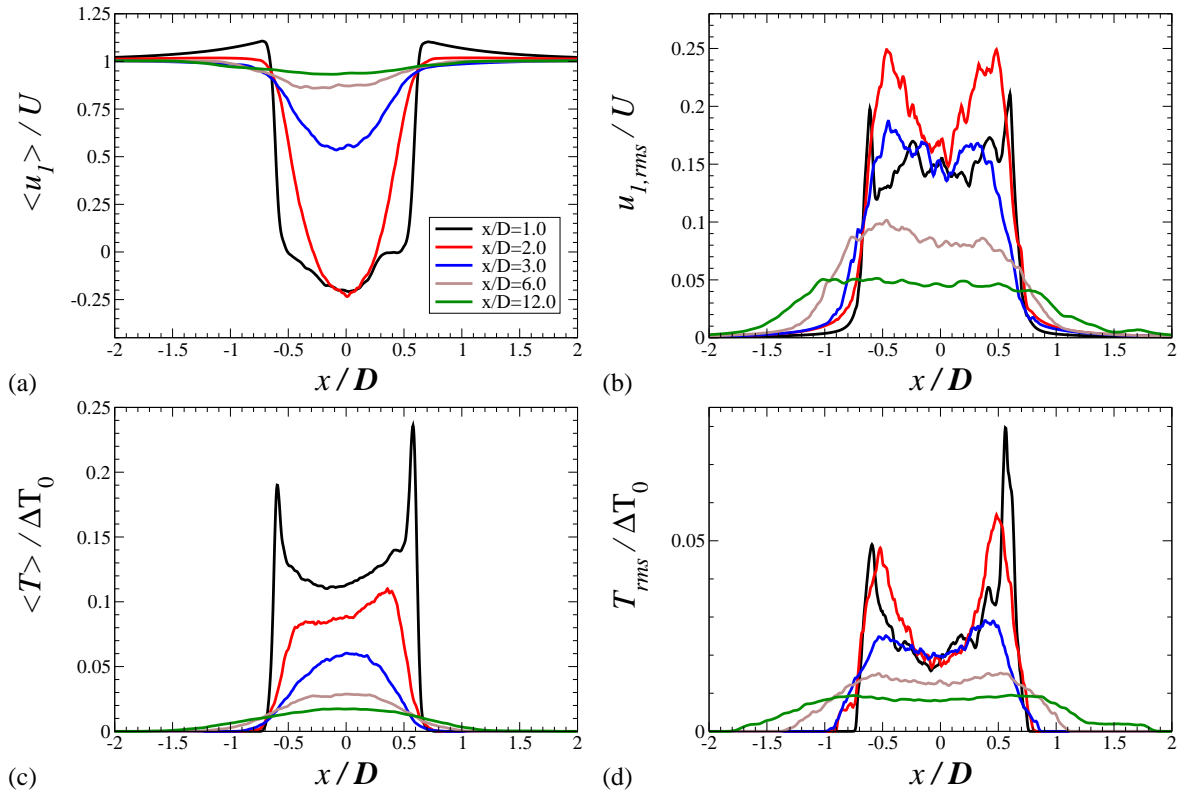


Figure 3: Mean and root mean square profiles in the wake. (a) Mean streamwise velocity. (b) RMS streamwise velocity. (c) Mean temperature. (d) RMS temperature.

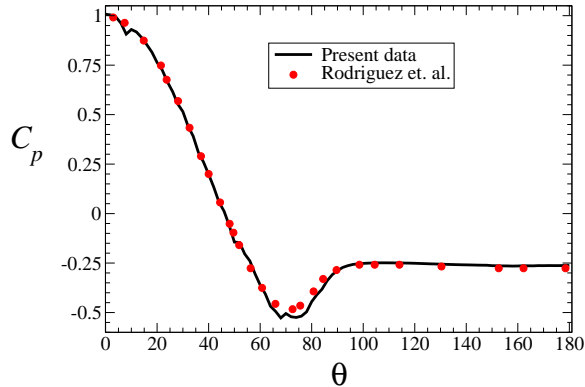


Figure 1: Mean pressure coefficient around the sphere. Data from the $Re = 10,000$ DNS of Rodriguez *et al.* (2013) is shown for comparison.

scale L_f is given by

$$L_f^2(t) = 2 \frac{\int_A (x_\alpha - x_\alpha^c)^2 f^2 dA}{\int_A f^2 dA}, \quad x_\alpha^c(t) = \frac{\int_A x_\alpha f^2 dA}{\int_A f^2 dA}, \quad (1)$$

with α representing a given coordinate direction and f representing the variable of interest. Note that for the mean streamwise velocity, the wake dimensions are calculated based on the wake defect velocity. The wake dimensions presented here were calculated from the 1D average of the $x_1 - x_3$ and $x_1 - x_2$ planes.

For analyzing the wake dimensions we will break the wake into two pieces. The first is for the re-circulating re-

gion with $x_1/D < D/2 + L_r = 2.224$. In this region the obtained wake dimensions are much larger for the mean temperature field than the mean velocity field. This occurs due to the dominance of the large temperature value in the separated shear layer which is located far from the vertical centerline. Similarly to the larger mean temperature value, the temperature fluctuations are larger in the re-circulating region than the velocity fluctuations.

The second region occurs after the re-circulating region, $x_1/D > 2.224$. We will refer to this region as the developed region. In the developed region, the dimensions of the temperature and velocity fields are comparable for both the mean and fluctuating fields. The values for the temperature and velocity fields differ by 10%. It is interesting to note that the mean velocity field is 10% larger than the mean temperature field but that the fluctuating temperature field is 10% larger than the fluctuating velocity field. Dmitrenko *et al.* (1986a) observed a fixed ratio of 1.2 for both $L_{u_{1,rms}}/L_{\langle u_1 \rangle}$ and $L_{T_{rms}}/L_{\langle T \rangle}$. Here we observed that both $L_{u_{1,rms}}/L_{\langle u_1 \rangle}$ and $L_{T_{rms}}/L_{\langle T \rangle}$ are approximately constant in the developed region but the values are different with $L_{u_{1,rms}}/L_{\langle u_1 \rangle} \approx 1.4$ and $L_{T_{rms}}/L_{\langle T \rangle} = 1.63$. The growth rate in the developed region was found to be nearly identical for the mean and fluctuating values at approximately $x^{1/2}$. This value is larger than the value of $x^{1/3}$ expected in the self-similar regime.

Conclusions

To the best of the author's knowledge, this study is the first numerical attempt to simulate scalar mixing in the wake of a sphere with a turbulent wake. Visualizations of the temperature and vorticity field show a link between the coherent

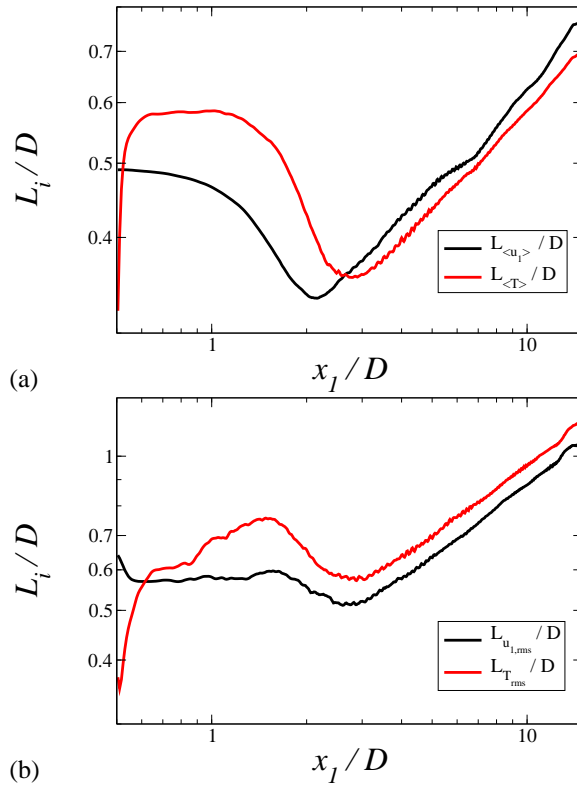


Figure 4: Wake dimensions based on (a) Mean velocity and temperature. (b) RMS velocity and temperature.

structures in the velocity field and temperature fluctuations. The separated shear layer carries large values of the temperature away from the hot sphere and into the cold fluid. Mixing is enhanced by the Kelvin-Helmholtz shear instability which causes rollers to form which engulfs cold fluid into the hot region.

Profiles of the mean and fluctuating fields were provided at five locations in the wake. These profiles show the strong role played by the separated shear layer in the near wake evolution. In particular, large fluctuating values of the velocity and temperature are found at off center peaks in the region behind the separated shear layers. The values for the wake dimensions were found to be within 10% for the velocity and the temperature field in the developed region behind the re-circulating region. A constant power law was obtained for the growth rate with the same value of approximately $x^{1/2}$ obtained for the mean and fluctuating fields.

Simulations and analysis are currently ongoing. We plan to report more detailed results in a future publication.

ACKNOWLEDGMENTS

M.B.S. and S.S are pleased to acknowledge the support of the Office of Naval Research (ONR) Grant No. N0014-11-10469, program monitor Ron Joslin. M.B.S. also received support on this project from an Achievement Rewards for College Scientists Scholarship. Computational resources were provided by the Department of Defense High Performance Computing Modernization Program. All simulations were run on Diamond, an SGI Altix ICE 8200 LX at the US Army Corps of Engineers Engineering Research and Development Center.

REFERENCES

- Achenbach, Elmar 1974 Vortex shedding from spheres. *J. Fluid Mech.* **62** (02), 209–221.
- Berajeklian, A. & Mydlarski, L. 2011 Simultaneous velocity-temperature measurements in the heated wake of a cylinder with implications for the modeling of turbulent passive scalars. *Phys. Fluids* **23** (5), 055107.
- Brucker, K. A. & Sarkar, S. 2010 A comparative study of self-propelled and towed wakes in a stratified fluid. *J. Fluid Mech.* **652**, 373–404.
- Cometta, Carl 1957 An investigation of the unsteady flow pattern in the wake of cylinders and spheres using a hot-wire probe. PhD thesis, (Sc.M.)—Brown University., Also cited as Tech. Rep. WT-21.
- Constantinescu, George & Squires, Kyle 2004 Numerical investigations of flow over a sphere in the subcritical and supercritical regimes. *Phys. Fluids* **16** (5), 1449–1466.
- Constantinescu, G. S. & Squires, K. D. 2003 LES and DES investigations of turbulent flow over a sphere at $Re = 10,000$. *Flow, Turbulence and Combustion* **70**, 267–298.
- Dmitrenko, Yu.M., Zhdanov, V.L. & Kolovandin, B.A. 1986a Turbulent velocity and temperature fields in the nonisothermal wake behind an elongated body of revolution. *Journal of engineering physics* **50** (1), 9–15.
- Dmitrenko, Yu.M., Zhdanov, V.L., Kolovandin, B.A. & Labuda, I.A. 1986b Temperature fluctuation balance in an axisymmetric turbulent wake. *Journal of engineering physics* **50** (2), 123–128.
- Douglas, J. 1962 Alternating direction methods for three space variables. *Numerische Mathematik* **4**, 41–63.
- Freythuth, Peter 1975 Search for the final period of decay of the axisymmetric turbulent wake. *J. Fluid Mech.* **68**, 813–829.
- Freythuth, Peter 1976 Modeling of the final period of decay for the axisymmetric turbulent temperature wake. *Phys. Fluids* **19** (10), 1475–1477.
- Freythuth, Peter & Uberoi, Mahinder S. 1973 Temperature fluctuations in the turbulent wake behind an optically heated sphere. *Phys. Fluids* **16** (2), 161–168.
- Gibson, C. H., Chen, C. C. & Lin, S. C. 1968 Measurements of turbulent velocity and temperature fluctuations in the wake of a sphere. *AIAA J.* **6** (4), 642–649.
- Matsumura, M. & Antonia, R. A. 1993 Momentum and heat transport in the turbulent intermediate wake of a circular cylinder. *J. Fluid Mech.* **250**, 651–668.
- Parnaudeau, Philippe, Carlier, Johan, Heitz, Dominique & Lamballais, Eric 2008 Experimental and numerical studies of the flow over a circular cylinder at Reynolds number 3900. *Phys. Fluids* **20** (8), 085101.
- Piquet, Jean & Vasseur, Xavier 2000 A nonstandard multi-grid method with flexible multiple semicoarsening for the numerical solution of the pressure equation in a navier-stokes solver. *Numerical Algorithms* **24**, 333–355.
- Rhie, C. M. & Chow, W. L. 1983 Numerical study of the turbulent flow past an airfoil with trailing edge separation. *AIAA J.* **21** (11), 1525–1532.
- Rodriguez, I., Lehmkuhl, O., Borrell, R. & Oliva, A. 2013 Flow dynamics in the turbulent wake of a sphere at subcritical Reynolds numbers. *Comput. Fluids* **80** (0), 233 – 243.
- Roman, F., Napoli, E., Milici, B. & Armenio, V. 2009 An improved immersed boundary method for curvilinear grids. *Comput. Fluids* **38** (8), 1510 – 1527.
- Schmid, M. & Peric, M. 2001 Large eddy simulation of subcritical flow around sphere. In *High Performance*

August 28 - 30, 2013 Poitiers, France

- Computing in Science and Engineering 2000* (ed. Egon Krause & Willi Jager), pp. 368–376. Springer Berlin Heidelberg.
- Williamson, J. H. 1980 Low-storage Runge-Kutta schemes. *J. Comput. Phys.* **35**, 48–56.
- Yun, Giwoong, Kim, Dongjoo & Choi, Haecheon 2006 Vortical structures behind a sphere at subcritical Reynolds numbers. *Phys. Fluids* **18** (1), 015102.
- Zang, Y., Street, R. & Koseff, R. 1994 A non-staggered grid, fractional step method for time-dependent incompressible Navier-Stokes equations in curvilinear coordinates. *J. Comput. Phys.* **114**, 18–33.